JOTCS A
Journal of the Turkish Chemical Society
Section: A
Chemistry
TURKISH CHEMICAL SOCIETY

Activated Plantain Peel Biochar As Adsorbent For Sorption of Zinc(II) Ions: Equilibrium and Kinetics Studies.

***Nworie F. S[1], Nwabue F[1]. Ik, Ikelle I. I[1]., Ogah A.O[1]., Elom N[1]; Illochi, N.O[2], Itumoh E.J[1]. and Oroke C.E[1]**

[1]Department of Industrial Chemistry, Ebonyi State University, Abakaliki, Nigeria.
[2]Department of Pure Chemistry Evangel University, Akaeze, Ebonyi State, Nigeria.

Abstract: Plantain peel biomass was carbonized, activated, and characterized using BET surface area and XRD. The XRD diffraction indicated crystalline structure with crystallite size of 14.56 nm evaluated through Debye-Scherrer equation. The pore size (cc/g) and pore surface area (m^2/g) of the biochar was 8.79 and 16.69 respectively from BET surface area. Various parametric properties such as effect of initial metal ion concentration, pH, and contact time were studied in a batch reaction process. Adsorption of zinc from aqueous solution decreased with an increase of pH and initial concentration. Equilibrium modeling studies suggested that the data fitted mainly to the Langmuir isotherm. Adsorption kinetic data tested using various kinetic models fitted the Bangham's pore diffusion model implicating pore diffusion as the main rate limiting step. The sorption studies indicated the potential of plantain peel biochar as an effective, efficient and low cost adsorbent for remediating zinc (II) ions contaminated environment.

Keywords: biochar, zinc (II) ions, adsorption and kinetic models, plantain peel

Submitted: June 28, 2018. **Accepted:** October 30, 2018.

Cite this: Nworie F, Nwabue F, Ikelle I, Ogah A, Elom N, Illochi N, et al. Activated Plantain Peel Biochar As Adsorbent For Sorption of Zinc(II) Ions: Equilibrium and Kinetics Studies. JOTCSA. 2018;5(3):1257–70.

DOI: http://dx.doi.org/10.18596/jotcsa.438332.

***Corresponding author. E-mail:** nworie.felix@gmail.com; Phone: +2348034813342.

INTRODUCTION

Biomass from decaying plant or other agricultural remnants can be converted to biochar which is important in carbon sequestration, and averting global climate change. Consequently in recent years, the use of agricultural biomass to create biochar has given promising results in carbon dioxide reduction (1). Biochar as an important soil amender is a carbon-rich charcoal that is produced by the thermal decomposition of agricultural biomass. Biochar obtained from the pyrolysis of readily accessible biomasses such as organic, industrial and agricultural wastes has been proved to be an effective and efficient means of carbon sequestration and immobilization of organic contaminants in soil adsorbent (1,2). Specifically, plantain peels have been noted to exert effects on clinically important agents and are important as good adsorbent (1,3-5) .

The wastes from plantain constitute serious environmental hazard as they are most of times carelessly disposed leading to clogging of waterways and converting the town centers to foul smelling scenes. Peels of plantain are wastes and are shown to be a very good source of phyto-chemicals and dietary fibers which are beneficial to human body (6).

Trace metals occur in aqueous solutions from two main sources which could be pedogenetic involving

weathering of parent materials in which case it is less than 1000 mg/kg and less or rarely toxic and from anthropogenic sources such as smelting, electroplating, mining energy and fuel production, agricultural activities and other industrial and commercial activities (7). The last sources and especially the mining and land filling sites are the major contributor of trace metals to aqueous media. Trace metal ions always regarded as those metals with relatively high density and are deleterious even at low concentrations is major environmental contaminants and poses threat to human life and animal wellbeing (8).

Some studies (9,10) have noted that trace metals are non-degradable and continuous accumulation leads to increase in contamination of coastal waters and estuaries. Similarly, these heavy metals bioaccumulate in tissues and organs of biotas adversely affect the distribution of marine organisms. Zinc is a heavy metal highly essential for both plants and animals (8) but becomes deleterious at excess concentration. Zinc from anthropogenic sources such as sludge application, industrial activities and mining, wastewater sources can easily contaminate the environment and present itself as serious threat to man, animals and soil (11). Zinc toxicity is mainly in the form of free zinc(II) ions and the bioavailability and toxicity of the zinc(II) ions can be reduced by immobilization process using biomaterials without adverse effect to the ecosystem.

The removal of soluble metal ions from aqueous solution by the use of biochar has been currently advocated for as it is gradually replacing the expensive materials such as complexing agents and activated carbon (10). Source of biomass and variation of conditions of biochar production are factors that influence biochar characteristics (12). Previous studies on the use of biochar from variety of biomasses for sorption of zinc(II) ions are limited as well as expansive equilibrium and kinetic studies. In other to explore the sorption mechanism of zinc(II) ions and influence of sorption conditions of time of contact, pH, initial metal ions concentration and provide useful data for biochar usability, this study was conducted. The main focus was on the synthesis of the plantain peel biochar, its characterization, metal sorption studies at different conditions of pH, time of contact and initial zinc(II) ions concentration, mechanism of adsorption and the equilibrium and kinetics of the adsorption of zinc onto activated plantain peel biochar.

MATERIALS AND METHODS

Materials

Analytical grade reagents H_2SO_4, HNO_3, NaOH, Na_2CO_3, Eriochrome black-T, EDTA, NaCl, $ZnSO_4$ were all obtained from Sigma Aldrich® and used without further purification unless indicated. Double distilled water was used for all experiments.

Characterization of the activated plantain peel biochar

The BET surface area was measured using Micromeritics ASAP 2020 system. X-ray diffraction pattern was obtained on a Bruker® D8 Discover diffractometer, equipped with a Lynx Eye detector, under Cu-Ka radiation (l ¼ 1.5405 Å). With data collected in the range of 2θ =10 to 100 °, scanning rate at $0.010^{o}min^{-1}$,192 s per step and samples placed on a zero background silicon wafer slide.

Sample Collection and Preparation

The unripe plantain peels *(Musa paradisiaca)* was collected from Abakaliki metropolis in Ebonyi state of Nigeria in plastic containers. The samples after collection were cleaned of soil and other impurities, sun dried to reduce moisture content for 7 days and then oven dried at 60 °C for 24 h. The modified method (13) was adopted for carbonization of the plantain peels. This was done at a temperature of 600 °C in nitrogen environment in a muffle furnace for 6 h. The resulting biochar was cooled at room temperature, ground to fine powder, and then subjected to activation. A portion of 10 g of the carbonized biochar was measured into a 500 mL beaker and 30 mL of concentrated HNO_3 added with stirring for 2 h continuously. The mixture was diluted with deionized water and decanted several times and then washed with double distilled water until the pH was tested to be 6.5. The activated biochar was then dried in an oven at a temperature of 110 °C.

EXPERIMENTAL

Adsorption of Zinc(II) Ions by batch process

Batch experiments were done to obtain adsorption data by varying different conditions of time of contact, pH and initial metal ion concentration. The adsorption of zinc(II) ions from aqueous solution was investigated by initially adding 0.1 g of the adsorbent to 10 mL 0.01 M Zn(II) ions aqueous solution in a 500 mL vessel at room temperature (30 ± 1 °C) for 120 min. The solution was equilibrated using mechanical shaker and resulting solution filtered. The isotherm and kinetics experiments helped to elucidate the characteristics and mechanism of zinc sorption onto the activated plantain peel biochar. For each experiment, 0.1 g of the activated biochar was mixed with 10 mL zinc solution in the vessel. The mixture was shaken at 100 rpm on a rotary mechanical shaker at room temperature. Consequently to measure the sorption kinetics, 0.01 M zinc solutions were used and time varied between 10-120 seconds. To get sorption isotherms, 0.1 g of the activated biochar was added to different concentrations of zinc

solution (0.1, 0.2, 0.3, 0.4 M) and the mixture equilibrated for 120 seconds. Similar method was applied for pH varied between 2-10. The mixtures were separated by filtration using Whatman No1 filter paper at the end of each experiment. The method (14) was used for the determination of zinc left in the solution after adsorption. To determine the concentration of zinc in the filtrate, Equation 1 was used.

$$Concentration\ of\ Zinc\ in\ solution = \frac{Molarity\ of\ EDTA \times Volume\ of\ EDTA}{Volume\ of\ zinc\ solution} \quad \text{(Eq. 1)}$$

The complexation of EDTA with zinc is represented in Equation 2 indicating 1: 1 number of moles of each reactant involved.

$$Zn^{2+} + EDTA^{4-} \rightarrow ZnEDTA^{2-} \quad \text{(Eq. 2)}$$

The amount of zinc adsorbed per unit mass of adsorbent at equilibrium, (qe) (mg/g) was evaluated using the relation in Equation 3.

$$qe = \frac{Co}{Ce} \times \frac{V}{M} \quad \text{(Eq. 3)}$$

where Co is initial concentration of zinc(II) ions in solution, Ce is the equilibrium concentration of zinc(II) ions, V is the volume of the solution and m the mass of the activated plantain peel adsorbent.

RESULTS AND DISCUSSION

XRD analysis of the solid sorbent

The diffraction pattern of activated plantain peel biochar (Figure 1) showed crystalline nature with significant intense peak observed at 2θ = 40.65 with observed decomposition of some compound after forming the biochar of plantain peels (15,16). The crystallite size (nm) was calculated from Debye-Scherrer equation(Equation 4):

$$d = \frac{K\lambda}{\beta Cos\theta} \quad \text{(Eq. 4)}$$

Where K is Debye-Scherer constant, β is the full width at half maximum, is the wavelength and θ is Bragg angle. The average crystal size of the particles as calculated from the width of the XRD peaks using Debye-Scherrer equation was 14.56 nm indicating that the biochar is nanosized (17).

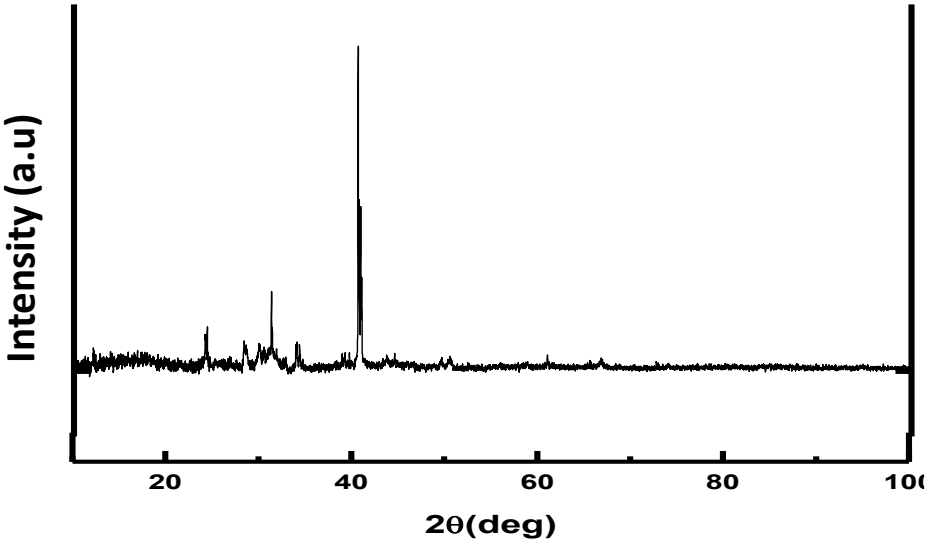

Figure 1: X-ray diffractogram of activated plantain peel biochar.

Brunauer, Emmett, Teller (BET) surface area characterization

BET surface area was applied to determine the surface area and pore size of the plantain peel biochar. The pore size (cc/g) and pore surface area (m^2/g) of the biochar was 8.79 and 16.69 respectively and represented in Figure 3. The large surface area per gram of a sample of the biochar indicates that there is less erosion and more ability to capture metallic particulates present in a given media (18). BET surface area analysis and XRD analysis of the biochar showed nanosize forms of the biochar typical of a nanocrystalline material (12).

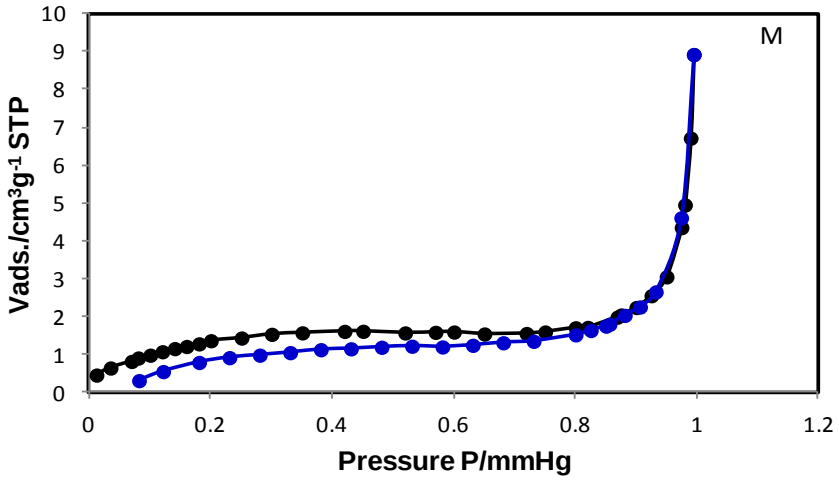

Figure 2: BET surface area plot of activated plantain peel biochar.

Batch Experiments

pH influence

Data obtained for the influence of pH on the sorption of zinc(II) ions on batch equilibration are plotted as shown in Figure 3. The adsorbent consumption of zinc(II) ions as shown in Figure 3 was highly influenced by the variation of the pH of the solution. As the pH of the solution was varied from 2 to 10, there was observed decrease of adsorbed zinc (II) ions from the equilibration mixture. At higher pH, the observed decrease in adsorption could be as the result of basic dissociation of active sites of the adsorbent forming positively charged species on the solid which interfered with the metal adsorption or due to the anionic surface of the biochar at lower pH promoting increased metal ion uptake (13).

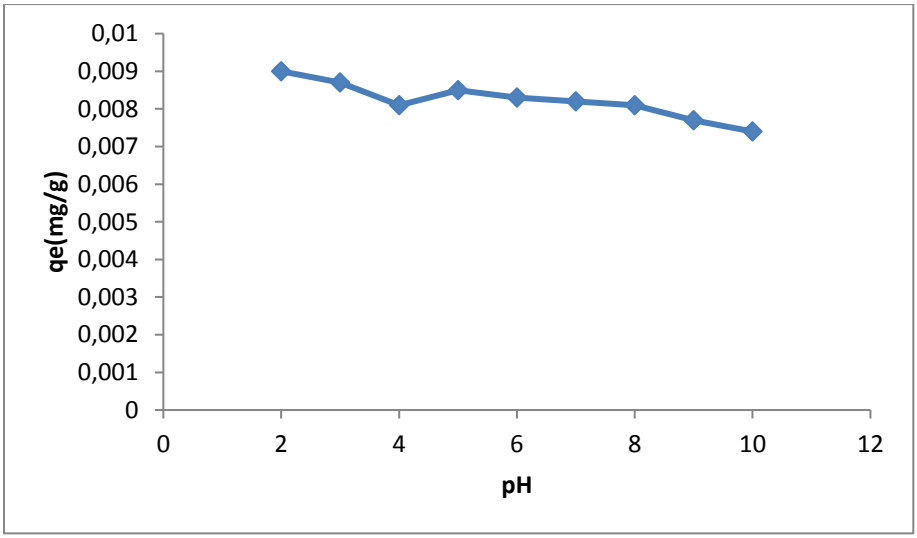

Figure 3: Effect of the initial pH of solution on equilibrium adsorption capacity of activated plantain peel biochar.

Effect of time of contact

Adsorption increased with increase in time of contact as shown in Figure 4. The plot of the variation of zinc(II) ions adsorbed against time of contact shown in Figure 4 indicated that the adsorption increased with time of contact until equilibrium was reached. This means that as adsorption starts, there are active sites available which got occupied and co-ordinatively consumed with increased time thereby clogging the sorption sites and a reduction or unavailability of free site. This observation is in line with the study (11) on the removal of prevalent heavy metals ions by sorption on scots pine and silver birch biochar.

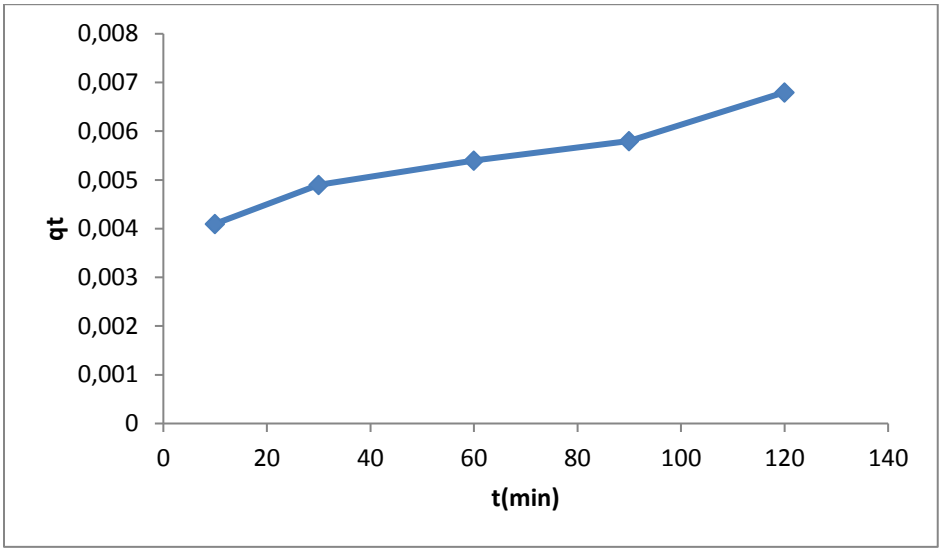

Figure 4: Effect of time of contact on the adsorption of zinc (II) ions on activated plantain peel biochar (pH = 6.5; initial metal ion concentration = 0.01 M).

Effect of initial metal ion concentration

The equilibrium stage sorption of the zinc(II) ions is plotted against the initial concentration of the sorptive solution as shown in Figure 5. There is enhanced sorption of zinc(II) ions at lower sorptive concentration which decreased linearly with increase in sorptive concentration. This observation could be that as concentration of zinc(II) ions increased, active adsorption sites get adsorptively saturated leading to decrease in adsorption efficiency. The observation could as well be as a result of increased active centres available at higher dilutions for relatively smaller amount of the sorbing ions (13,19,20). This is also in line with the study (14) which reported on the determination of zinc using EDTA complexometric studies. The sorption efficiency was high and the mechanism of the removal of zinc(II) ions from solution could be surface electrostatic interaction, cation exchange, precipitation or surface complexation (4,11,21). Based on the equilibrium and kinetic result for the simulated data, sorption capacity increased as initial concentration increased. Thus, fractional adsorption of zinc (II) ions increased as initial concentration increased until at equilibrium and intraparticle mechanism primarily involving surface electrostatic interaction, cation exchange, precipitation or surface complexation could be in operation. Kinetic model explanation as given under Weber and Morris intraparticle diffusion and Bangham's pore diffusion model clearly explained that both mechanisms could be in operation based on the fitting of the simulated data. Similarly, increase in pH leads to decrease in negative charges on biochar due to decrease in negative sites. This led to decreased adsorption as electrostatic attraction was decreased and surface functional group dissociation could be responsible for alteration of adsorption.

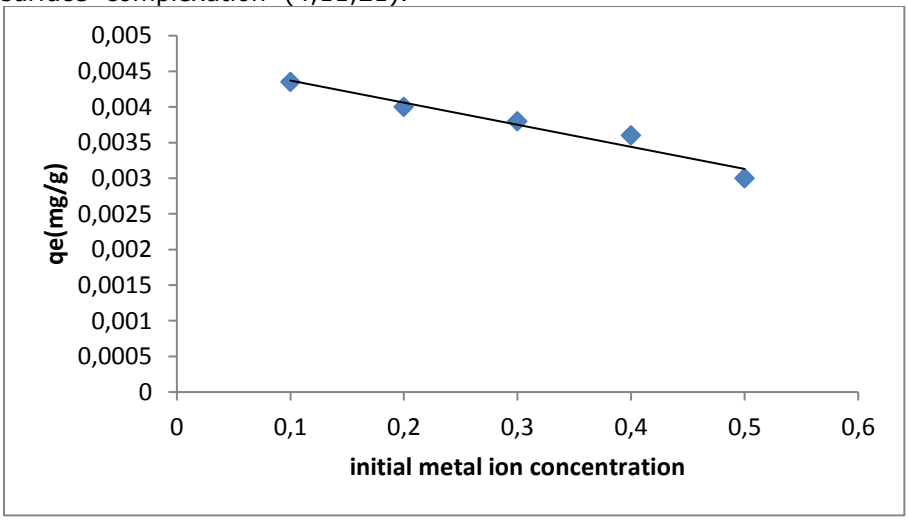

Figure 5: Effect of zinc (II) ions initial concentration on the adsorption onto activated plantain peel biochar(pH =6. 5; contact time = 120 min).

Equilibrium Adsorption Isotherms

(1) Langmuir isotherm

The Langmuir adsorption isotherm considers adsorption to take place on homogenous site and ceases as sites become unavailable. The adsorption is thus monolayer without established interaction between the adsorbate (22,23). Langmuir model is expressed with Equation 4.

$$qe = Q_m \frac{bCe}{1} + bCe \quad \text{(Eq. 4)}$$

Ce(mg/g) is the concentration of adsorbate at equilibrium, q_e (mg/g) the mass of adsorbate, Qm and b are constants regarded as Langmuir constants and stands for maximum adsorption capacity and adsorptive bonding energy respectively determined graphically by linearizing Langmuir isotherm as shown in Equation 5a.

$$\frac{Ce}{qe} = \frac{Ce}{Qm} + \frac{1}{bQm} \quad \text{(Eq. 5a)}$$

Qm and b are constants from the graphical plot of $\frac{Ce}{qe}$ against Ce and represented as slope and intercept determined as 490 and -1,111 respectively. The Langmuir constant Qm was very high indicating a very strong affinity for zinc. From Figure 6, the correlation coefficient (R^2) equals 1 indicating a perfect fit of the monolayer adsorption. This indicates that the adsorption sites are energetically identical and equivalent, structurally homogeneous and no observed interaction between the molecules adsorbed and close sites. Transfer of the adsorbate from the available sites to another is inhibited in the surface of the sites and the plantain peel biochar has finite adsorptive capacity for the zinc(II) ions. To evaluate the dimensionless separation factor a measure of the desirability and favourability of the model, the Langmuir parameter b regarded as Langmuir isotherm model constant was employed and values optimized from Hall equation (Equation 5b) (23).

$$RL = \frac{1}{1+bCo} \quad \text{(Eq. 5b)}$$

Where Co is the initial concentration of zinc (II) ion and the values of b was found to be between 0 and I indicating the favorability of the adsorption process (23).

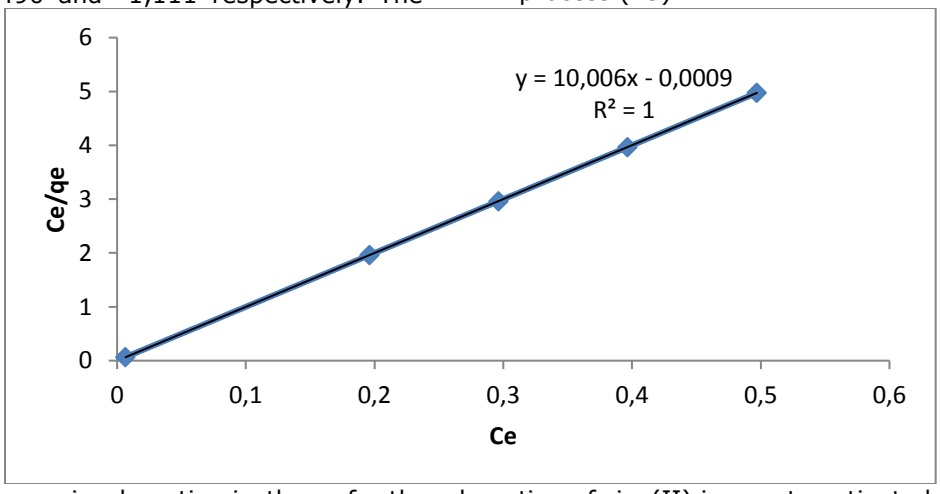

Figure 6: Langmuir adsorption isotherm for the adsorption of zinc(II) ions onto activated plantain peel biochar.

(2) Freundlich Isotherm

Freundlich sorption isotherm model considers the adsorption to occur in a heterogeneous surface where there is no limited degree of adsorption with sites and energies exponentially distributed (22,23). As expressed in Equation 6, n is the adsorption intensity and K_f the adsorption capacity obtained as the intercept and slope respectively and shown as the linear plot of In qe against In Ce illustrated in Equation 7. The values of n and K_f are -3.544 and 9.65 respectively. This shows that the Freundlich adsorption process is not favorable as the value of n is not within 1- 10 (23, 24.25, 26, 27, 28). The value of correlation coefficient was 0.8665 from Table 1 and Figure 7 indicating that the Langmuir isotherm simulated the data better (12).

$$qe = K_F Ce^{1/n} \quad \text{(Eq. 6)}$$

$$\text{In}q_e = \text{In}Kf + \frac{1}{n} InCe \quad \text{(Eq. 7)}$$

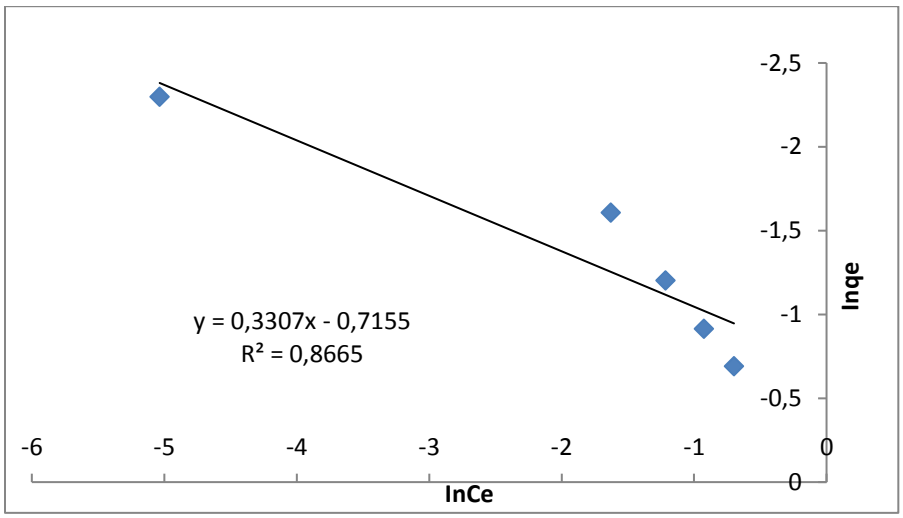

Figure 7: Freundlich adsorption isotherm for the adsorption of zinc(II) ions onto activated plantain peel biochar.

(3) Temkin isotherm

This considers the fall in the heat of sorption of molecules in the layer to decrease linearly with area of coverage owing to sorbent or sorbate interaction instead of logarithmic (22,23). The linear form of Temkin isotherm model is shown in Equation 8.

$$q_e = \beta \mathrm{In} A_t + \beta InCe \qquad \text{(Eq. 8)}$$

β is related to the heat of sorption and A is the binding constant at equilibrium state. The plot of q_e versus In C_e gives the slope and intercept as A_t and β respectively. From Table 1 and Figure 8, the value of R^2 (0.6898) is less than Langmuir and Freundlich isotherms but greater than that of Elovich model. The values of A_t and β are 2161.47 and -68.87 respectively indicated weak affinity of the sorbate confirming that the model could not explain explicitly the sorption process.

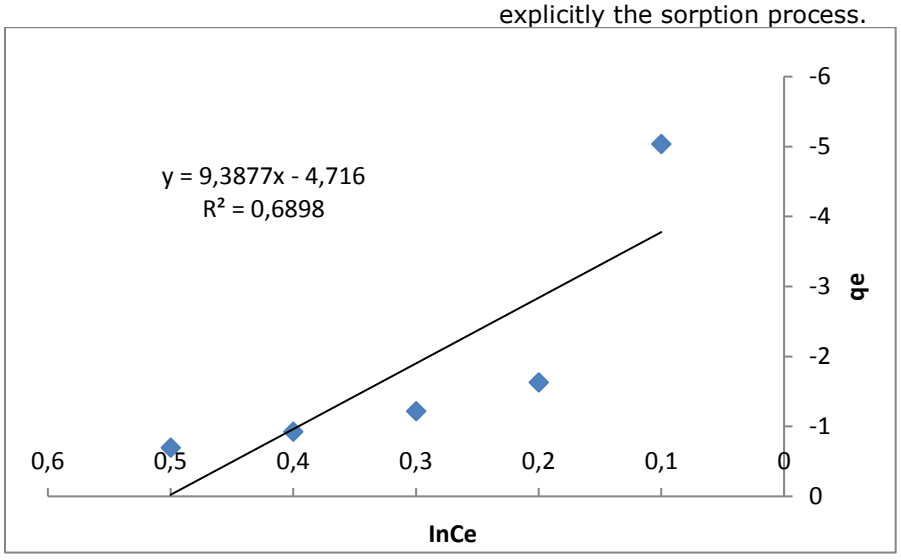

Figure 8: Temkin adsorption isotherm for the adsorption of zinc(II) ions onto activated plantain peel biochar.

(4) Elovich isotherm

Elovic isotherm model describes a multilayer sorption process (23,24) that exponentially increase with adsorption site. The isotherm is represented in Equation 9:

$$\frac{\mathrm{qe}}{\mathrm{qm}} = K_E Ce^{e^{\frac{qe}{qm}}} \qquad \text{(Eq. 9)}$$

Elovich maximum sorption capacity and sorption constant Km and K_E respectively are evaluated from the slope and intercept of the plot of In (q_e/C_e) versus q_e to be 115.62 and 591.78. As shown in Table 1 and Figure 9, the value of R^2 is 0.5039 which is less than Langmuir, Freundlich and Temkin isotherms illustrating that the adsorption does not fit the Elovich isotherm model. The low value of the sorption capacity confirms the monolayer adsorptivity and defies the fact that the sorption is multilayer (23,24).

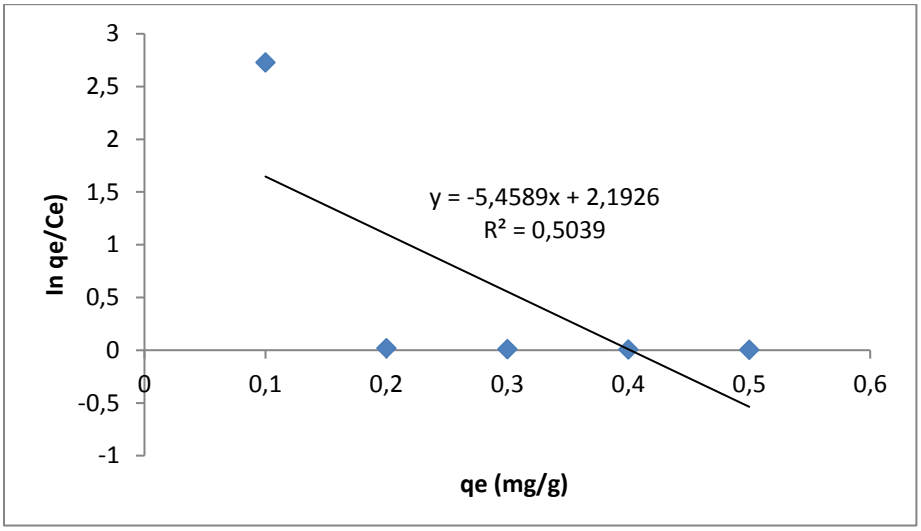

Figure 9: Elovich sorption isotherm for the adsorption of zinc(II) ions onto activated plantain peel biochar.

Adsorption Kinetics

Different parametric adsorption kinetics models were used to analyze the adsorption processes.

Pseudo-first- order model

The sorption of adsorbate from liquid phase is considered and this remains the most widely used Lagergren's rate equation (24).

$$\ln(qe - qt) = \ln qe - k_1 t \quad \text{(Eq. 10)}$$

Equation 10 shows the linearized pseudo-first order model with t as time of contact, qt is mass of zinc(II) ions, qe is equilibrium mass of zinc(II) ions adsorbed, K_1 pseudo first order constant. As shown in Table 1 and Figure 10, the data have low regression coefficient of 0.8143 and low value of K_I of -0.0376 showing that the sorption process does not agree with the model.

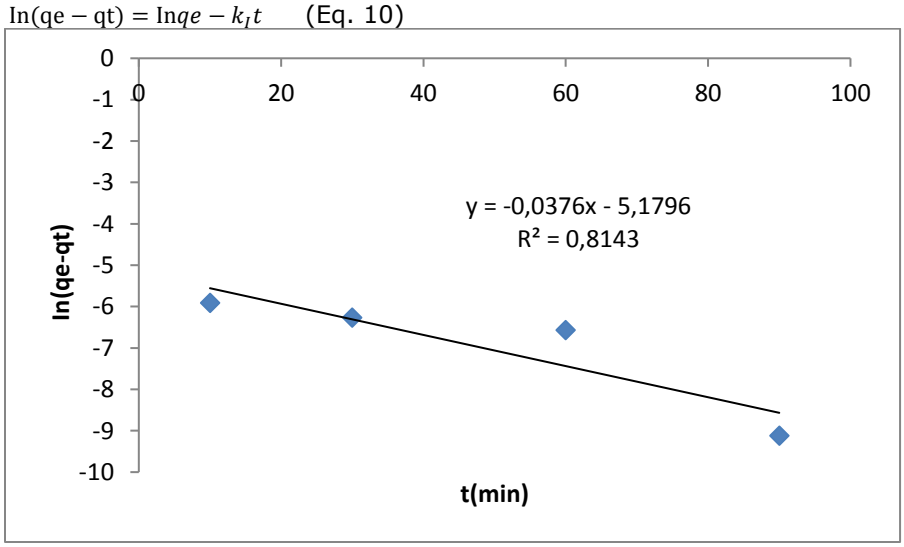

Figure 8: Pseudo-first –order kinetic plot for the adsorption of zinc(II) ions onto activated plantain peel biochar.

Pseudo-second-order kinetic model

Chemisorption defines the rate-controlling step in pseudo-second-order process as illustrated in Equation 11 (12).

$$t/qt = 1/K_2\, qe^2 + t/qe \quad \text{(Eq. 11)}$$

Where K_2 is pseudo second order constant. The obtained data of R^2 (0.9773)(Figure 9) indicates a good relationship between the parameters and shows that the adsorption kinetic model could be in control of the process. The value of K_2 was 71.42 high enough but lower than Bangham's pore diffusion model and indicated that chemisorption could be part of the rate-determining step.

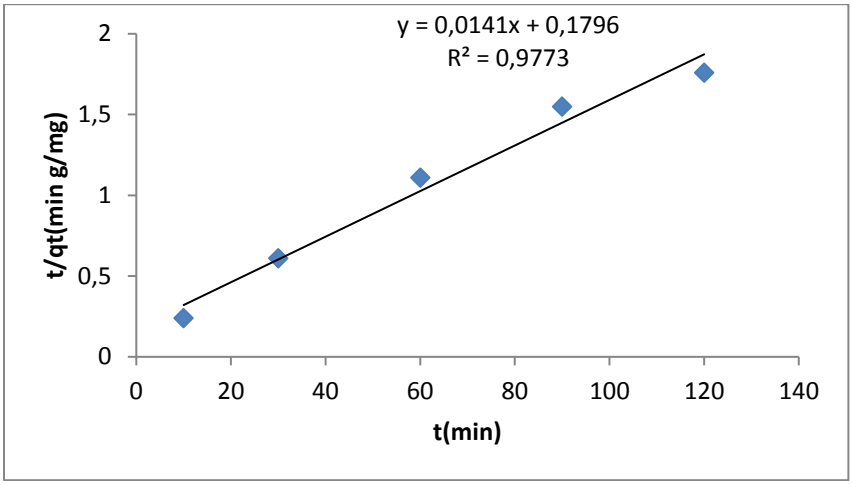

Figure 9: Pseudo -second –order kinetics plot for the adsorption of zinc(II) ions onto activated plantain peel biochar.

Elovich kinetic model

Elovich model describes the kinetics of chemisorption of gas and or solute onto solid sorbents and represented in Equation 12 (12,19).

$$q_t = \frac{1}{\beta}\ln(\alpha\beta) + \frac{1}{\beta}In(t) \qquad \text{(Eq. 12)}$$

The constants ą and β represents the initial adsorption rate (mg/gmin^{-1}) and the degree of surface coverage and activation energy for chemisorption (g/mg) respectively. These values were obtained from the slope and intercept of the linearized plot of q_t against In t (12,23) as 0.001 and 0.0017, respectively. From Table 1 and Figure 10, the regression coefficients of the data was high and good fitting (R^2 =0.903). The values obtained suggested that diffusion could be part of the rate determining step and accounted for the parameters in Elovich model a confirmation that chemisorption could be part of the rate-limiting step. Chakrapani *et al* (24) in his study made similar observation and maintained that the equation prevails at situations where the rate of desorption is negligible.

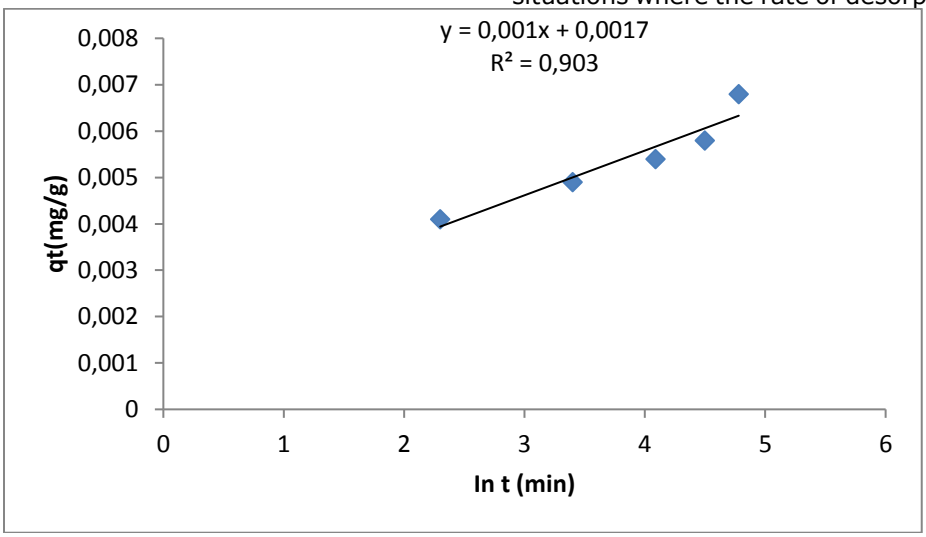

Figure 10: Elovich kinetics plot for the adsorption of zinc(II) ions onto activated plantain peel biochar.

Weber and Morris intraparticle diffusion model

The linear form of Weber and Morris intraparticle diffusion model is shown in Equation 13 (25,26).

$$qt = K_I t^{1/2} + C \qquad \text{(Eq. 13)}$$

Where K_I (slope) is intraparticle diffusion rate constant (mg/g min$^{1/2}$) and C the intercept representing the sorption strength of the boundary layer calculated from the linear plot of qt against $t^{1/2}$ as 0.003 and 0.0031 respectively with high regression coefficient (R^2) of 0.9584. A high value of C indicates high sorption capacity (25) and justifies the extent of intraparticle diffusivity of the adsorbate through the adsorbent surface. From Figure 11, the plot is linear but never passed through the origin indicating that intra particle diffusion could be among the mechanistic steps but

not the only rate determining process. The failure of the intercept line to go through the origin could be as the result of the differences in mass movement of adsorbate in the beginning and ending processes of the sorption implicating boundary layer control in the adsorption (26).

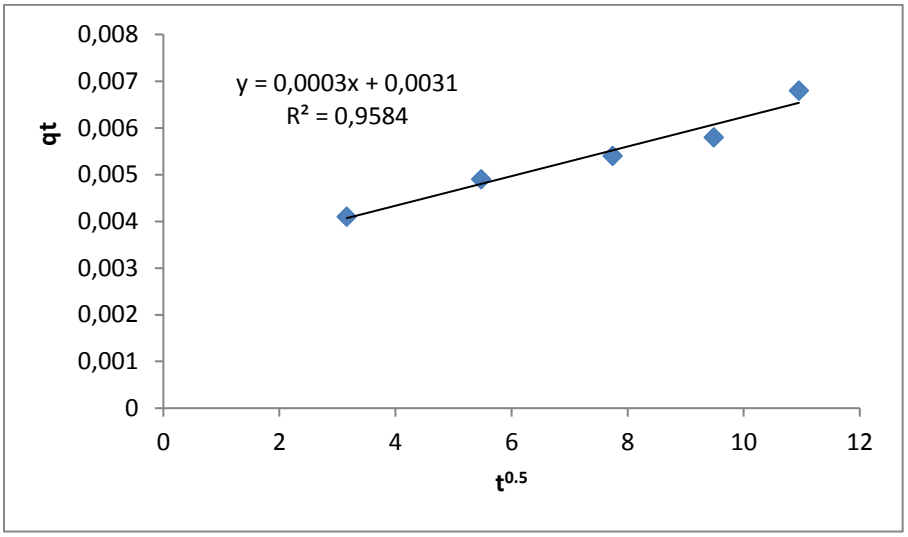

Figure 11: Weber and Morris intraparticle diffusion model for the adsorption of zinc(II) ions onto activated plantain peel biochar.

Liquid film diffusion kinetic model

Diffusion is controlled by liquid films in contact with the adsorbent and represented in Equation 14 (12).

$$In(1-\frac{qt}{qe}) = -K_{lf}t \qquad \text{(Eq. 14)}$$

A plot of ln $(1-\frac{qt}{qe})$ versus t gave the slope as K_{lf} representing the liquid diffusion constant regarded as the external mass transfer coefficient (1/min). Figure 13 gave the slope as 0.0002 with poor regression coefficient (R^2) of 0.7478. The result confirms that the sorption is not liquid film diffusion dependent and this was strongly in agreement with the study of Panida and Xianshe (26).

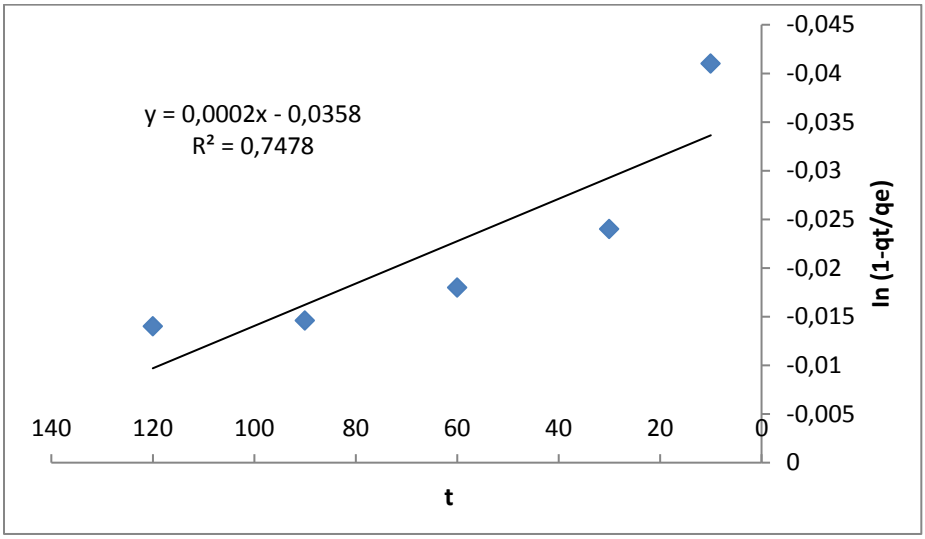

Figure 12: Liquid film diffusion model for the adsorption of zinc(II) ions onto activated plantain peel biochar.

Bangham's pore diffusion model

Linearized Bangham's pore diffusion model is represented in equation 15 (25).

$$\text{Log log}\left\{\frac{\text{Co}}{Co-mqt}\right\} = \text{Log}\left\{\frac{\text{m}K_B}{2.303V}\right\} + \delta\beta logt \qquad \text{(Eq. 15)}$$

Where Co is the initial zinc(II) ion concentration (mg/L), V is solution volume (mL), m the weight of adsorbent(g/L), dβ and K_B are constants representing the slope and intercept obtained from linearized plot of log log [Co/Co-mqt] versus log t. The plot as shown in Figure 13 is linear with high regression coefficient (R^2) of 0.992 indicating that the kinetic model confirmed the Bangham equation and that pore diffusion processes are prevalently in control of the sorption of zinc(II) ions onto plantain peel biochar(24).

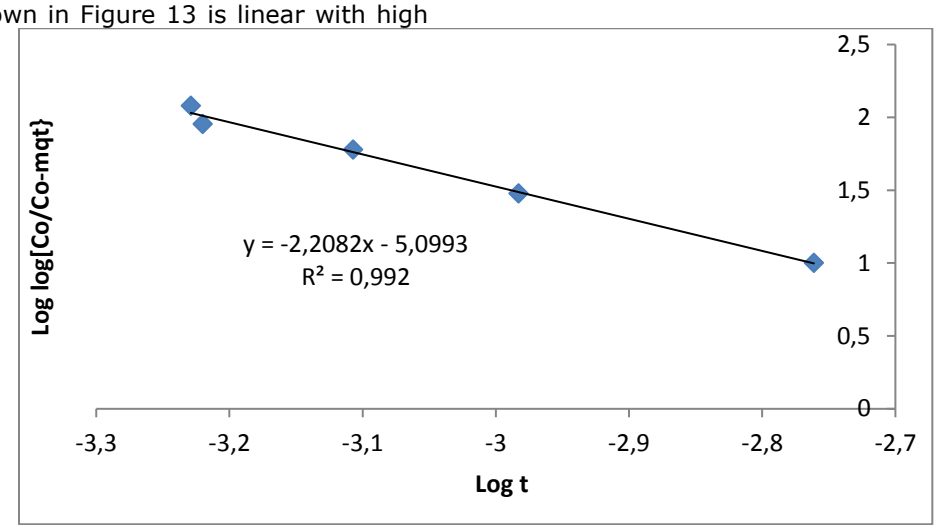

Figure 13: Bangham's pore diffusion model for the adsorption of zinc(II) ions onto activated plantain peel biochar.

Table 1: Equilibrium and kinetic model parameters for the adsorption of zinc(II) ions on activated plantain peel biochar.

S/N	Models	Parameter 1 K_f(mg/g)	Parameter 2 qe(mg/g),b(L/mg)	R^2
	Kinetic models			
1	Pseudo-First order	$K_{1\ =}$ -0.0376	q_e = -5.1796	0.8143
2	Pseudo-second order	K_2 = 71.42	q_e = 0.1796	0.9773
3	Elovich	α = 0.001	β = 0.0017	0.903
4	Weber and Morris intraparticle	K_I =0.003	C = 0.0031	0.9584
5	Liquid film diffusion	K_{lf} =0.0002	qe =-0.0358	0.7478
6	Bangham pore diffusion	dβ =-2.208	K_B = -5.099	0.992
	Equilibrium models			
7	Langmuir	q_m = 490.00	b = -1,111	1
8	Freundlich	K_f = 9.65	n = -3.544	0.8665
9	Temkin	A_t =2161.47	B = -68.87	0.6898
10	Elovich equation	Km = 115.62	K_E= 591.78	0.5039

CONCLUSION

The presence of Zn(II) ion from aqueous media was removed by adsorption using an effective, efficient and low cost plantain peel biochar. XRD analysis of the biochar indicated that it is of nanosize form corroborating the BET surface analysis of pore size and pore surface area typical of a nanocrystalline material. Zinc(II) ions sorption increased with increase in time until equilibrium at 120 minutes but decreased with increase in pH and initial zinc(II) ion concentration. Sorption equilibrium and kinetic models were applied to test the effectiveness, efficiency and applicability of the processes. The adsorption isotherm obeyed Langmuir monolayer process whereas the kinetic mechanism showed mainly pore diffusion process been prevalent. The study serves as a green approach to the removal of zinc(II) ions from contaminated media. The method is green because it sequestrates metal contaminants from the environment without contaminating the environment. A green or benign analytical approach is an environmentally friendly approach for which the adsorption process presents. The zinc metal can be eluted or desorbed from the activated plantain peel biochar for reuse or before discarding to the environment as a soil amender.

REFERENCES

1. Oberio HS, Vadlani P V, Saida L, Hughes J D. Ethanol production from plantain peels using statistically optimized simultaneous

saccharification and fermentation process. Waste Management. 2011; 31: 1576-85.

2. Onyebado CO, Iyagba ET, Offor OJ. Solid soap production using plantain peels ash as source of alkali. Journal of Applied Science and Environmental Management.2004; 6**:** 73-7.

3. Mitani N, Jian FM. Uptake system of silicon in different plant species. J. Exp. Bot. 2005; 56 (414): 1255–61.

4. Uchimiya M, Chang S, Klasson KT. Screening biochars for heavy metal retention in soil: Role of oxygen functional groups. J. Haz. Mat. 2011; 190 (1-3): 432-41.

5. Betiku E, Sheriff O A. Modeling and optimization of Thevetiaperuviana (yellow oleander) oil biodiesel synthetic via Musa paradisiacal (plantain) peels as heterogeneous base catalyst: A case of artificial neural network vs. response surface methodology. Ind. crop. prod. 2014; 53: 314-22.

6. Wolfe K, Wu K, Liu RH. Antioxidant activity of apple peels. J. Agric. Food Chem. 2003; 51:609-14.

7. Ismail S, Khan F, Zafar- Iqbal M. Phytoremediation: Assessing tolerance of tree species against trace metal (Pb and Cd) toxicity. Pakistan J Botany. 2013; 45: 2181-6.

8. Parizanganeh AH, Bijnavand V, Zamani AA, Hajabolfath A. Concentration, distribution and comparison of total and bioavailable trace metals in top soils of Bonab district in Zanjan province. Open J. Soil Sci. 2012; 2: 123-32.

9. Dada AO, Ojediran JO, Olalekan AP. Sorption of Pb^{2+} from aqueous solution unto modified rice husk: isotherm studies. Adv Chem Phys. 2013: 1–6 (id: 842425).

10. Babel S, Kurniawan TA. Low-cost adsorbents for heavy metals uptake from contaminated water: a review. J Hazard Mater. 2003; 97(1–3): 219–43.

11. Komkiene J, Baltrenaite E. Biochar as adsorbent for removal of heavy metal ions [Cadmium(II), Copper (II), Lead(II), Zinc(II) from aqueous phase. Int. J. Environ. Sci. Technol. 2016; 13: 471-82.

12. Inyang M, Cao B, Pullammannappallil P, Zimmerman A R. Enhanced lead sorption by biochar derived from anaerobically digested sugarcane bagasse. Sep. Sci. Technol. 2011; 46(12): 1950-6.

13. Tiwari LD, Lee S. Activated carbon and manganese coated activated carbon precursor to dead biomass in the remediation of arsenic contaminated water. Environmental Engineering Research. 2012; 17:541-8**.**

14. Prasad AS. Zinc deficiency by global health organization. British Medical Journal. 2003; 326 (7386): 409-10.

15. Jindapon W, Jaiyen S, Ngamcharussrivichai C. Al_2O_3-supported Mixed Ca and Zn Compounds Prepared from Waste Seashells for Synthesis of Palm Fatty Acid Methyl Esters, Chemical Engineering Communications. 2015; 202: 1591–9.

16. Morin TJ, Chengeto SW, Makura V, Tatlock HM, Lindeman SV, Bennett B, Long GJ, Grandjean F, Gardinier JR. Pyrazolylmethyls prescribe the electronic properties of iron(II) tetra(pyrazolyl)lutidine chloride complexes, Dalton Trans. 2011; 40: 8024–34.

17. Zhou Y, Gao B, Zimmerman AR, Cao X. Biochar-supported zerovalent iron reclaims silver from aqueous solution to form antimicrobial nanocomposite. Chemosphere. 2014; 117: 801-5.

18. Demirbas A. Effects of temperature and particle size on biochar yield from pyrolysis of agricultural residues. Journal of Analytical and Applied Pyrolysis. 2003; 72: 243-8.

19. Thavamani SS, Rajkumar R. Removal of Cr(II), Pb(II) and Ni(II) from aqueous solution by adsorption on alumina. Res. J. Chem. Sci. 2013; 3(8): 44-8.

20. Okareh OT, Adeolu AT. Removal of Lead ion from industrial effluent using plantain wastes. Br. J. App. Sci. Technol. 2015; 8(3): 267-276.

21. Cao XD, Ma L, Gao B, Harris W. Dairy manure derived biochar effectively sorbs lead and atrazine. Environ. Sci. Technol. 2009; 43(9): 3285-91.

22. Mazhar IK, Saima QM, Sajida P, Muhammed YK. Citrus paradise: An effective bio-adsorbent for arsenic(V) remediation. Pak. J. Anal. Environ. Chem. 2014; 15(1): 35-41.

23. Farouq R, Yousef NS. Equilibrium and Kinetics Studies of Adsorption of Copper (II) Ions on Natural Biosorbent. Int. J. Chem. Eng. Appl. 2015; 6: 319-24.

24. Chakrapani CH, SureshBabu CH, Vani KNK, Somasekhara Rao K. Adsorption kinetics for the removal of fluoride from aqueous solution by activated carbon adsorbents derived from the peels of selected citrus fruits.. E- journal of chemistry. 2010; 7(SI): S419-27.

25. Antonija k, Natlija V, Dam H, Davor K. Lignocellulosic materials as dye adsorbents: Adsorption of methylene blue and congo red on brewers spent grain. Croat. Chim. Acta, 2018; 91: 53-64.

26. Panida S, Xianshe F. Kinetic models on chromium(VI) adsorption onto carbonized oil palm kernel with potassium hydroxide activation. Intl J. Adv. Chem. Eng. Biol. Sci. 2016; 3(1): 68-75.

27. Erol K. The adsorption of calmoduline via nicotinamide immobilized poly(HEMA-GMA) cryogels. JOTCSA. 2017; 4(1): 133-48.

28. Yildiz A. Adsorption of Acid Red 114 onto Fe_3O_4 at Caffeic acid recyclable magnetic nanocomposite. JOTCSA. 2017; 4(1): 327-40.